J Mater Sci (2009) 44:3255–3264
DOI 10.1007/s10853-009-3437-4

New route to process uni-directional carbon fiber reinforced $(SiC + ZrB_2)$ matrix mini-composites

**N. Padmavathi · K. K. Ray · J. Subrahmanyam ·
P. Ghosal · Sweety Kumari**

Received: 1 December 2008 / Accepted: 23 March 2009 / Published online: 15 April 2009

Abstract Unidirectional carbon fiber-reinforced $(SiC + ZrB_2)$ matrix mini-composites were prepared by soft solution route. In this process, the matrix materials were prepared using water-soluble precursors of colloidal silica, sucrose, zirconium oxychloride, and boric acid as sources of silica, carbon, zirconia, and boron oxide respectively. The room temperature mechanical properties were investigated and the fracture features of the composites were examined. Tensile strength of 269 ± 36 MPa and fracture energy of 0.38 ± 0.05 MJ/m^3 for the mini-composite, carbothermally reduced at 1,600 °C were attributed to the fiber pull out. In spite of a composite failure mode, the composite carbothermally reduced at 1,700 °C exhibited lower mechanical properties. It showed that carbon fibers reacted with ZrO_2 to form ZrC phase at 1,700 °C, formed chemical bonding, and led to a strong interface between fibers and matrix, which resulted in the degradation of mechanical properties of the mini-composites. The XRD and SEM investigations of the powders and the mini-composites revealed phase formation whereas cross-sectional microstructure indicated the uniform distribution of fibers within the matrix.

N. Padmavathi (✉) · J. Subrahmanyam · P. Ghosal ·
Sweety Kumari
Ceramics Composites Group, Defence Metallurgical Research
Laboratory, Kanchanbagh, Hyderabad 500058, Andhra Pradesh,
India
e-mail: nandigam_padma@rediffmail.com;
nandigam_padma@yahoo.com

N. Padmavathi · K. K. Ray
Department of Metallurgical and Materials Engineering,
Indian Institute of Technology, Kharagpur 721302, India

Introduction

Continuous carbon-fiber-reinforced SiC matrix composites (C_f–SiC) are promising structural candidates for advanced applications, such as heat shields and structural components for re-entry space vehicles, high-performance brake discs, and ultra-high temperature heat exchanger tubes, due to their potential for providing excellent mechanical properties at high temperatures [1]. In order to improve the mechanical properties as well as oxidation resistance of C_f–SiC composites at elevated temperatures, zirconium-based ceramics have demonstrated a wide range of attributes [2, 3]. Particularly, zirconium diboride (ZrB_2) is a material of interest because of the excellent and unique combination of high melting point (3,050 °C), high electrical and thermal conductivity ($\sim$60 W/mK^2), good thermal shock resistance, high strength (565 MPa), and excellent resistance to chemical attack [4, 5]. $SiC + ZrB_2$ ceramics, of suitable composition are known to have better combination of strength and oxidation resistance, than monolithic ZrB_2. Addition of ZrB_2 enhances the oxidation resistance of SiC by promoting the formation of a protective borosilicate glass layer. $SiC + ZrB_2$ ceramic composites have thus become viable candidates for various ultra-high temperature aerospace applications [6].

Several processing methods, such as chemical vapor infiltration (CVI), polymer impregnation and pyrolysis (PIP), sol–gel, slurry infiltration followed by hot pressing, and in situ chemical reaction techniques, have been employed for fabricating continuous fiber-reinforced ceramic composites [7–9]. Each processing method has its advantages and disadvantages pertaining to reproducibility, cost, and performance of the composite. New processing techniques are desirable to meet the demands of high performance and low cost. The soft-solution approach using low-cost materials such as colloidal silica, zirconium oxychloride, boric acid, and sucrose. The processing conditions are so selected as to promote nanometer-scale mixing of different phases which can subsequently produce homogeneous ceramic powders as well as composites with any selected reinforcement; the matrix is formed in situ. The present method to synthesize mini-composites is simple and economical compared to the generally used sol–gel methods; it is a quite environmental-friendly approach, as it involves neither extremely low or high temperatures, nor toxic reagents [10, 11].

Synthesis of SiC + ZrB_2 composite powders requires selection of carbothermal reduction temperature and studying the phase formation. Unidirectional carbon-fiber-reinforced (SiC + ZrB_2) matrix composites are prepared by soft-solution approach by impregnating the solution phase into a carbon fiber tow, drying, converting sucrose into carbon phase, and finally reducing oxides with carbon to form silicon carbide and zirconium diboride. Processing, microstructure and mechanical properties of the mini-composites are mainly studied.

Experimental procedure

Carbon fiber tow was of T-300 grade (fiber vol%, 45) with 12,000 filaments in a tow; the filament diameter was about 6 μm. Commercial colloidal silica (SiO_2, 40 wt%, Bee Chem. Chemicals Company, Kanpur, India), boric acid (H_3BO_3, AR, Qualigens Fine Chemicals, India), zirconium oxychloride ($ZrOCl_2 \cdot 8H_2O$, AR, Loba Chemicals, India), and sucrose ($C_{12}H_{22}O_{11}$, AR, Qualigens Fine Chemicals, India) were used as source materials for silica (SiO_2), boron oxide (B_2O_3), zirconium dioxide (ZrO_2), and carbon, respectively, to prepare the powders as well as the mini-composites. SiC + ZrB_2 matrix forms by the carbothermal reduction of silica and (zirconia + boron oxide) at high temperatures. The precursor solutions with varying amounts of colloidal silica, sucrose, boric acid, and zirconium oxychloride were prepared. The amounts of the ingredients were calculated considering the following stoichiometric reactions involved for the preparation of mini-composites consisting of SiC + ZrB_2 as the matrix.

$$C_{12}H_{22}O_{11} \rightarrow 12C + 11H_2O \uparrow \tag{1}$$

$$2H_3BO_3 \rightarrow B_2O_3 + 3H_2O \uparrow \tag{2}$$

$$ZrOCl_2 \cdot 8H_2O \rightarrow ZrO_2 + 2HCl \uparrow + 7H_2O \uparrow \tag{3}$$

$$SiO_2 + 3C \rightarrow SiC + 2CO \uparrow \tag{4}$$

$$ZrO_2 + B_2O_3 + 5C \rightarrow ZrB_2 + 5CO \uparrow \tag{5}$$

The amounts of the ingredients are usually expressed in terms of molarity (a measure of concentration of a solution in number of moles of the solute per liter of solution). Typical calculations for the amounts of raw materials in molarities (mol/L, M) required for the preparation are summarized in Table 1. The precursor powders were prepared using the following three major steps: (1) the prepared precursor solutions were first dried at room temperature for at least 2 days, and then dried at 65 ± 5 °C for 12 h (2) the dried powders were ground and carbonized at 500 °C in argon atmosphere to convert sucrose into carbon, and finally (3) the carbonized powders were heated at 1,600 °C in argon atmosphere to reduce silica to SiC and $ZrO_2 + B_2O_3 + C$ to ZrB_2 by the carbothermal reduction. Initially, thermogravimetric analyses (Setsys 24 TG-DTA thermal analyser SETARAM, France) of dried green precursor powders were carried out to study mass change with temperature for evaluation of the carbothermal reduction temperature.

The desired nominal compositions of the mini-composites were SiC: 5 wt% ZrB_2, SiC: 10 wt% ZrB_2, SiC: 15 wt% ZrB_2, and SiC: 20 wt% ZrB_2. Initially, carbon fiber tow was washed with acetone to remove surface impurities and sizing. Then the fiber tows were vacuum impregnated with precursor solutions of (SiC + ZrB_2) as presented in Table 1. Impregnated tows were dried carefully at room temperature and at 60–70 °C for 12 h. Dried tows were carbonized at 500 °C under argon atmosphere for 1 h for converting sucrose into carbon. Evaporation of bonded water of zirconium oxychloride and decomposition of boric acid also occur during carbonization of sucrose. These steps were repeated for 5–6 cycles (further cycles were not required after completion of six cycles due to the rapidly decreasing effectiveness of further impregnation). After the desired impregnation/carbonization cycles, green composites were carbothermally reduced at 1,600 °C and 1,700 °C

Table 1 Amounts of the raw materials used for preparing the mini-composites, in moles

Composition (wt%)	Colloidal silica (M)	Sucrose (M)	$ZrOCl_2 \cdot 8H_2O$ (M)	Boricacid (M)
SiC + 5% ZrB_2	2.37	0.86	0.044	0.09
SiC + 10% ZrB_2	2.25	0.84	0.089	0.18
SiC + 15% ZrB_2	2.12	0.82	0.130	0.27
SiC + 20% ZrB_2	1.99	0.80	0.180	0.35

for 3 h under flowing argon to obtain the (SiC + ZrB_2) matrix. Flow sheet for the employed process is shown in Fig. 1.

Bulk densities and open porosity of the samples were determined by the Archimedes displacement method, and the estimation of theoretical density was based on the rule of mixture. The obtained products in powder form as well as the prepared mini-composites were subjected to X-ray diffraction (Philips Model No. PW 320) to identify the phases formed and to determine the crystallite size of the individual phases. It was difficult to prepare cross-sectional polished samples from the mini-composites. It was possible to view the microstructure of the composites by filling the porosity with a low-viscosity resin. Environmental scanning electron microscopy (ESEM, FEI, and QUANTA 400, Netherlands) was used to study the microstructure of the mini-composites.

In the mini-composite approach, single tows were impregnated along the fiber direction to get the composite. One of the benefits with the mini-composite approach was the better utilization of the expensive fiber material. The mini-tow composite samples can be stressed in uniaxial direction in tension, which gives more appropriate data, compared to flexure testing [12, 13]. Tensile tests were conducted using a servo-hydraulic testing machine (Model 8801; Instron Corp., UK) at room temperature under a displacement rate of 0.5 mm/min using 1 kN load cell. For each type of mini-composite, 10 tensile tests were carried out on specimens having constant gauge length and assuming that each mini-composite is having constant cross-sectional area (i.e., width = 0.657 mm, thickness = 0.657 mm, and area = 0.43 mm^2). Specimens were prepared with a gauge length of 50 mm and using paper tabs with a suitable adhesive for gripping according to the procedure outlined for mini-composites at room temperature by Naslain et al. [14]. Once the mini-composite sample was mounted on the machine, the cardboard tab supporting the composite was cut, and testing was carried out assuming constant cross-sectional area for each mini-composite. Weibull statistical analysis of the tensile data was carried out to get an idea of the scatter in the data [15]. The average values of tensile strength and fracture energy obtained from the area under the tensile curves were calculated from 10 specimens for each composition.

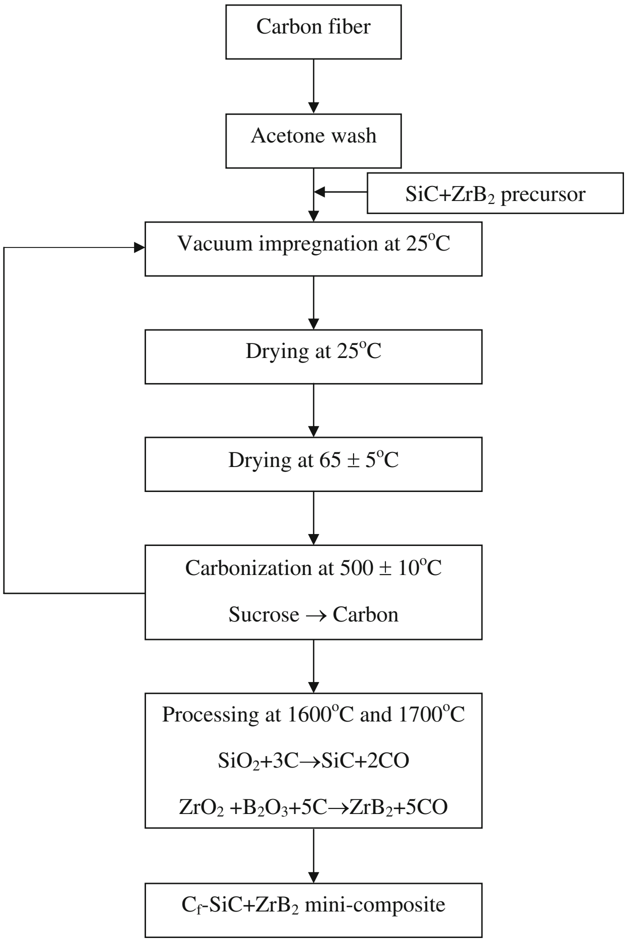

Fig. 1 Flow chart for the synthesis of carbon-fiber-reinforced SiC + ZrB_2 mini-composites using soft-solution approach

Results and discussion

Thermal analysis (TG, DTG and DTA) curves for ZrB_2 green powder are shown in Fig. 2. The TG curve shows that mass loss begins at lower temperature and continues up to 1,200 °C, rapid mass loss occurs between 1,200 °C and 1,527 °C, and beyond 1,527 °C mass loss is negligible. The considerable mass loss (~5%) and its corresponding inflection at 500 °C in DTG curve is due to dissociation and subsequent evaporation of the bonded water from zirconium oxychloride, decomposition of boric acid, and carbonization of sucrose. The mass loss associated with the

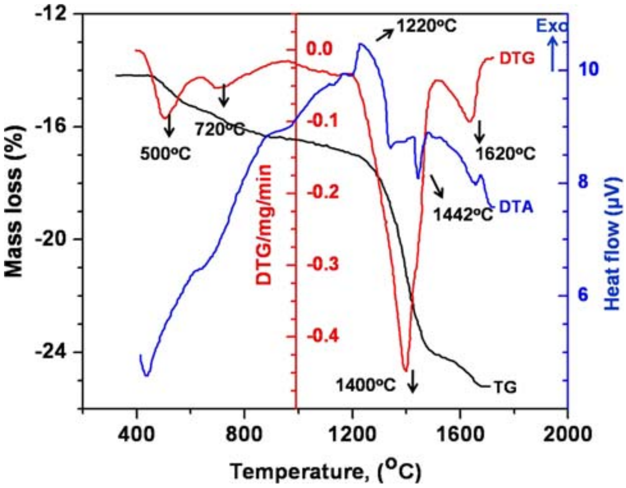

Fig. 2 Thermal analyses curve for the ZrB_2 precursor powder

reduction reaction of zirconia + boria is about 52.27% between 1,200 °C and 1,620 °C. For a stoichiometric mixture of zirconia + boria + carbon, the mass loss due to carbothermal reduction as per Eq. 5 should be 55.37%. The inflection at 720 °C is due to the continuous decomposition of zirconium oxychloride to amorphous zirconia and crystallization of amorphous zirconia to tetragonal zirconia [16]. The inflection in DTG curve at 1,400 °C is due to carbothermal reduction of zirconia + boria. The TG curve shows considerable mass loss whereas the DTA curve exhibits a weak endothermic peak at 490 °C; these are attributed to evaporation of bonded water from zirconium oxychloride and decomposition of boric acid. The endothermic peak at 1,220 °C indicates the onset of ZrB_2 formation. Two endothermic peaks are observed when carbothermal reduction leads to formation of pure ZrB_2. The endothermic peak at 1,442 °C is due to carbothermal reduction of $ZrO_2 + B_2O_3$ resulting in formation of ZrB_2 [17] and that at 1,642 °C can be attributed to the formation of ZrC.

Thermal analysis curves of SiC + 20% ZrB_2 green powder are shown in Fig. 3. TG curve shows that (i) mass loss begins at 100 °C and continues up to 1,200 °C, (ii) there is rapid mass loss between 1,227 °C and 1,627 °C, and (iii) the mass loss is negligible beyond 1,627 °C. TG analysis shows that considerable mass loss (5%) occurs up to 500 °C and this is due to the evaporation of bonded water and carbonization of sucrose. The mass loss associated with the reduction reaction of silica and zirconia is about 54.5% between 1,227 °C and 1,627 °C (TG curve). The DTG curve shows two inflections at 500 °C and at 1,521 °C. The inflection at 500 °C is due to the carbonization of sucrose, and decomposition of zirconium oxychloride and boric acid. The inflection at 1,521 °C is due to carbothermal reduction of silica and zirconia + boria as shown by Eqs. 4 and 5 [17]. However, in case of SiC + ZrB_2 precursor, only one inflection is observed at high temperature which indicates that both the oxides are reduced almost simultaneously. The endothermic peak at 1,181 °C indicates the onset of carbothermal reduction. The TG and the DTA curves show that considerable mass loss occurs at 1,521 °C coupled with an endothermic peak due to carbothermal reduction of silica + zirconia + boria to form SiC + ZrB_2. The TG curve of SiC + ZrB_2 precursor shows that the temperature for the formation of carbides gets shifted toward higher values relative to that for the ZrB_2 precursor.

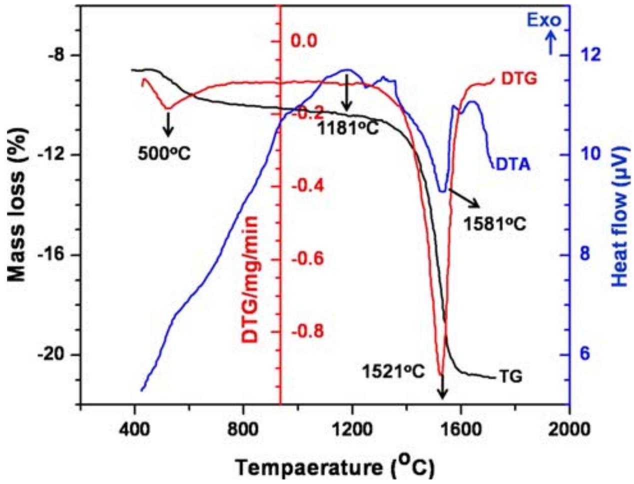

Fig. 3 Thermal analyses curve for the SiC + 20% ZrB_2 precursor powder

Thermodynamically, carbothermal reduction of silica occurs at 1,515 °C and that of zirconia + boria occurs at 1,497 °C, where the standard free energy changes (ΔG^0) for both the reactions are negative [18]. This shows that carbothermal reduction of $ZrO_2 + B_2O_3$ occurs at lower temperature compared to reduction of SiO_2 to give SiC. In this approach, SiO_2 gets transformed to SiC readily due to its amorphous nature making the latter to be the predominant phase in the product mixture at 1,521 °C; but substantial amounts of m-ZrO_2 and t-ZrO_2 remain present with the transformed ZrB_2. In general, the energy required to prepare borides (from B_2O_3), relative to the corresponding carbides, is greater per mass of boride product as a result of reducing the corresponding metal oxide in addition to reducing the required amount of B_2O_3 [19]. The endothermic peak at 1,581 °C can be attributed to the formation of ZrC [20]. The estimated values of mass loss and the temperatures suggest that carbothermal reduction can get completed at 1,500 <T> 1,800 °C for the powder mixtures. With this aim, two different temperatures of 1,600 °C and 1,700 °C have been selected to determine the influence of temperature on the properties of the mini-composites.

Figure 4 shows the XRD pattern of the composite powders which are carbothermally reduced at temperatures of 1,600 °C and 1,700 °C. The XRD results confirm the formation of β-SiC and ZrB_2 as the primary phases in the product. Figure 4a and b show peaks of both ZrB_2 and ZrC. The presence of additional phase ZrC in the final powder, prepared from $ZrO_2 + B_2O_3 + C$ system, indicates that the precursors are deficient in boron oxide content at higher temperatures. The boron oxide deficiency probably results from the high volatile nature of boron oxide. These observations are in agreement with the earlier results of TG-DTA, which indicated that high temperature is suitable for the reduction of untreated ZrO_2 to form ZrC. In XRD pattern of $ZrO_2 + B_2O_3 + SiO_2$ reaction mixture, as shown in Fig. 4c, SiC and relatively low-intensity ZrB_2 peaks are present together with that for the additional phase of ZrC. In case of pure ZrB_2 powder, there is no significant change in crystallite size (i.e., 84 nm) at different reduction

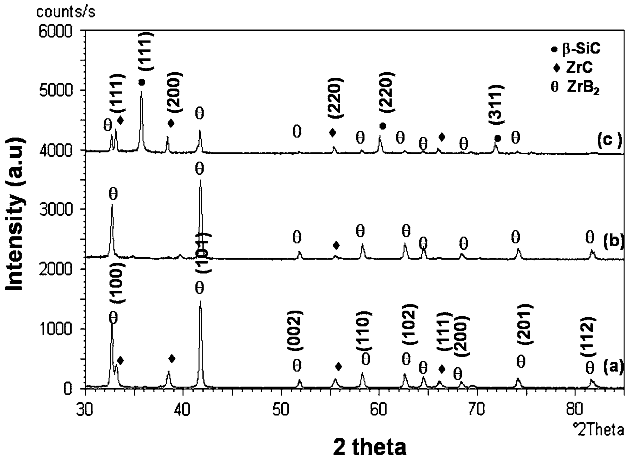

Fig. 4 XRD patterns of powders (a) ZrB_2 at 1,600 °C, (b) ZrB_2 at 1,700 °C, and (c) SiC + ZrB_2 at 1,600 °C

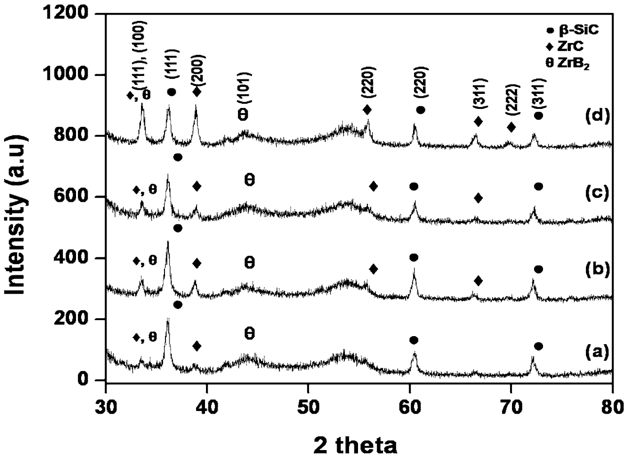

Fig. 6 XRD patterns of C_f–SiC mini-composites with (a) 5% ZrB_2, (b) 10% ZrB_2, (c) 15% ZrB_2, and (d) 20% ZrB_2 processed at 1,700 °C

temperatures. But in presence of SiC, the crystallite size of both ZrB_2 and SiC are 21.7 and 23.3 nm, respectively. The finer grain size can be explained by the fact that ZrB_2 grains are surrounded by SiC phase. This leads to the conclusion that formation of SiC hinders grain growth of ZrB_2. This will be useful in ultra-high temperature applications, as the grain-growth inhibitor would improve the material's stability at elevated temperature [6]. The small crystallite sizes and low temperatures to complete carbothermal reduction are indicative of the fine scale mixing of the reactants in the precursors. The initial solution allows homogeneous molecular level mixing of the ingredients and the crystallites of the product nucleate from amorphous phases.

Figures 5 and 6 show the XRD patterns of the mini-composites processed at 1,600 °C and 1,700 °C. The XRD patterns of the mini-composites exhibit peaks corresponding to β-SiC, ZrB_2, and ZrC phases together with minor peaks of graphite originating from the fiber. There is no trace of any unreacted SiO_2 or ZrO_2 in the diffraction patterns. The peak intensities for ZrB_2 increase with increase in ZrB_2 content in the matrix. The crystallite sizes of SiC and ZrB_2 in the mini-composites are presented in Table 2. The crystallite sizes of SiC and ZrB_2 in the mini-composites are found to be in the range of 20–40 nm. Crystallite size of SiC increased with decreased amount of SiC while the crystallite size of ZrB_2 decreased with increasing amount of ZrB_2 in the matrix. Crystallite sizes of both the phases increase with carbothermal reduction temperature. The presence of the fibers and the second phase are considered to hinder the growth of crystallites in the composites.

A typical microstructure of the composite prepared at 1,600 °C is shown in Fig. 7a, which indicates that the fibers are uniformly embedded in a densified matrix

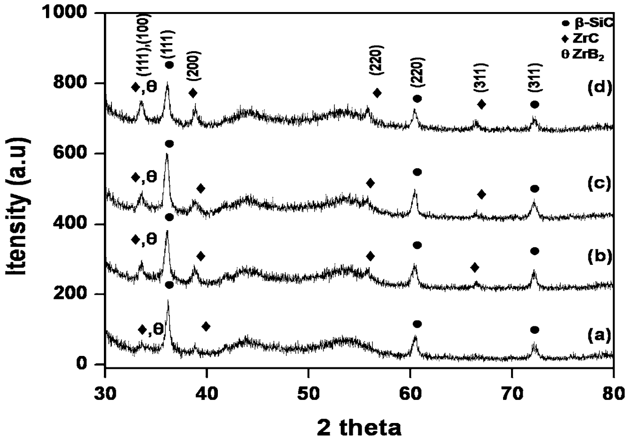

Fig. 5 XRD patterns of C_f–SiC mini-composites with (a) 5% ZrB_2, (b) 10% ZrB_2, (c) 15% ZrB_2, and (d) 20% ZrB_2 processed at 1,600 °C

Table 2 Crystallite sizes of SiC and ZrB_2 in the mini-composites at different processing temperatures

Composition (wt%)	Crystallite size (nm)			
	Carbothermal reduction temperature			
	1,600 °C		1,700 °C	
	SiC	ZrB_2	SiC	ZrB_2
SiC + 5% ZrB_2	24.8	30.1	25.4	35.5
SiC + 10% ZrB_2	24.4	26.0	24.3	31.4
SiC + 15% ZrB_2	23.7	24.8	24.0	29.5
SiC + 20% ZrB_2	22.0	23.3	23.1	26.3

The crystallite sizes of the SiC and ZrB_2 phases were calculated using the Scherrer equation, $D_{hkl} = K\lambda/\beta\cos\theta$, where K is a constant whose value is approximately 0.931, λ is the wavelength of X-ray, β is the width of the peak in degree (2θ) at ½ of maximum intensity, and θ is the Bragg angle

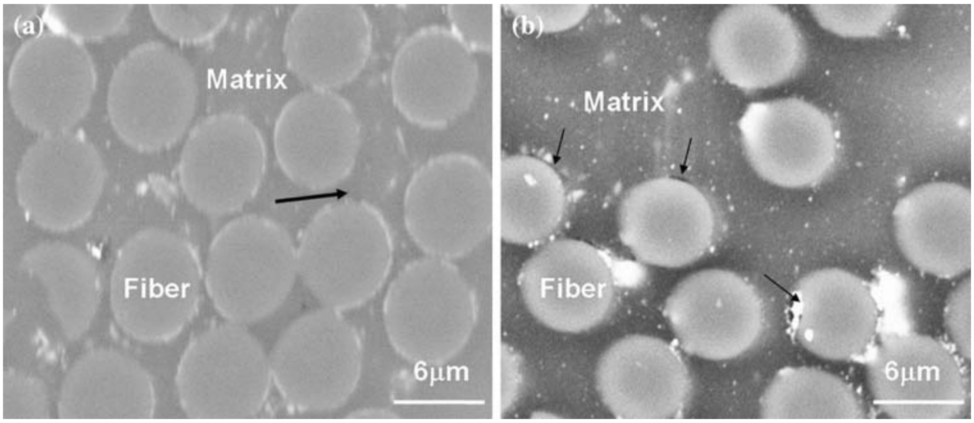

Fig. 7 ESEM image of carbon-fiber-reinforced SiC + 20% ZrB_2 mini-composites processed **a** at 1,600 °C and **b** at 1,700 °C

retaining their original shapes. The composites prepared at the temperature of 1,700 °C exhibit microstructure as shown in Fig. 7b, similar to that in Fig. 7a, and this observation infers that the employed fabrication process is suitable for the preparation of the mini-composites. A few fine cracks are found at fiber–matrix interface and some fiber damage (marked with black arrows) occurs during the process of fabrication, as shown in Fig. 7b. Figure 7b thus exhibits that the fibers in the composite, prepared at 1,700 °C, are in indirect contact with the matrix as revealed by the fiber–matrix interface. There exists evidence [20] that at temperatures above 1,650 °C, carbon fiber reacts with ZrO_2 to form ZrC at the interface of the fiber–matrix. Chemical reaction between fiber and matrix leads to the degradation of fiber properties with the surface of the fiber changing from groove marked to exfoliation, which influences the fracture process of the composites. This phenomenon may be attributed to the observed discrepancy in mechanical behavior of the mini-composites prepared at 1,600 °C and 1,700 °C.

Figure 8a shows the microstructure of the matrix of the C_f–SiC + 20% ZrB_2 mini-composite which shows fine grains of the different phases distributed over the matrix; Fig. 8b shows the corresponding back-scattered image. The microstructure in Fig. 8b shows that ZrB_2 (white phase) phase is well dispersed with SiC (dark phase) in the matrix. ZrB_2/ZrC phases are found to gather together to form large agglomerates, and in these agglomerates, the particle size of ZrB_2/ZrC is large (Table 2). The crystallite sizes of the synthesized matrix are in the range of 10–100 nm but usually exhibit agglomerated particle morphology with sizes ranging between 1 and 2 μm. In addition, large number of fine-grained crystallites of ZrB_2/ZrC are found distributed at the fiber–matrix interface in the composites, which indicates that carbon fiber reacts with ZrO_2 and then forms ZrC at the fiber–matrix interface.

Mechanical properties of unidirectional C_f–SiC + ZrB_2 mini-composites are presented in Table 3. Examination of the density data given in this table indicates that density of the composites increases with increase in the volume fraction of second phase (ZrB_2) in line with natural expectations, because this phase possesses higher density than that of SiC [11]. The relative density of the composites decreases with increasing percentage of ZrB_2. This might be due to the increase of viscosity with increase in the percentage of second phase which strongly suppresses the impregnation of solutions during processing. Porosity, on the other hand, increases with decrease in the volume

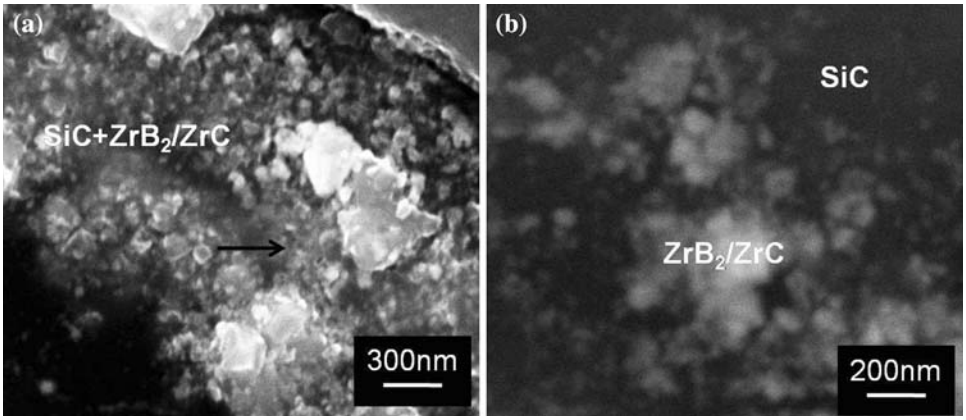

Fig. 8 **a** ESEM image of the matrix after processing and **b** corresponding backscattered SEM image of selected area of the matrix

Table 3 Mechanical properties of C_f–SiC + ZrB_2 mini-composites processed at 1,600 °C and 1,700 °C

Composition	Theoretical density (g/cm^3)	Bulk density (g/cm^3)	Relative density (%)	Failure load (N)	Tensile strength (MPa)	Fracture energy (MJ/m^3)	Weibull modulus (m)
At 1,600 °C							
SiC + 5% ZrB_2	1.94	1.67	85.6	96	155 ± 40	0.043 ± 0.01	3.7
SiC + 10% ZrB_2	2.13	1.72	80.8	118	245 ± 28	0.278 ± 0.05	8.2
SiC + 15% ZrB_2	2.24	1.77	79.0	124	247 ± 25	0.290 ± 0.11	9.3
SiC + 20% ZrB_2	2.30	1.78	77.4	141	269 ± 36	0.380 ± 0.05	7.3
At 1700 °C							
SiC + 5% ZrB_2	1.94	1.74	89.2	88	147 ± 35	0.09 ± 0.05	3.9
SiC + 10% ZrB_2	2.13	1.76	82.6	88	181 ± 17	0.23 ± 0.03	9.8
SiC + 15% ZrB_2	2.24	1.76	79.0	90	184 ± 24	0.18 ± 0.01	6.9
SiC + 20% ZrB_2	2.30	1.78	77.4	91	186 ± 42	0.19 ± 0.03	4.3

fraction of SiC. It can be further observed that the mini-composites, prepared at 1,700 °C exhibit comparatively poorer densification. The tensile strength and fracture energy are 269 ± 36 MPa and 0.38 ± 0.05 MJ/m^3, respectively for C_f–SiC + 20% ZrB_2 mini-composites prepared at 1,600 °C, while, tensile strength and fracture energy for the mini-composites are 186 ± 42 MPa and 0.19 ± 0.03 MJ/m^3, respectively when prepared at 1,700 °C. However, strength reduction is observed with increase in temperature for the carbothermal reduction i.e., from 1,600 °C to 1,700 °C.

It is well known that mechanical properties of fiber-reinforced ceramic composites depend not only on the properties of the fiber and the matrix or the processing conditions, but also on the characteristics of the fiber–matrix interface which play a major role in controlling the properties of these composites. In order to obtain high-performance ceramic matrix composites, desirable interfacial bonding is necessary to resist catastrophic failure caused by the matrix cracking through fiber bridging and pullout [21, 22]. Since similar matrices and processing conditions except for reduction temperatures are used for the preparation of all the composites, it is reasonable to assume that the discrepancy in mechanical properties resulting from the variation in reduction temperatures can be explained by the differences originating from the fiber–matrix interface, which depend primarily on the employed reduction temperature in this study.

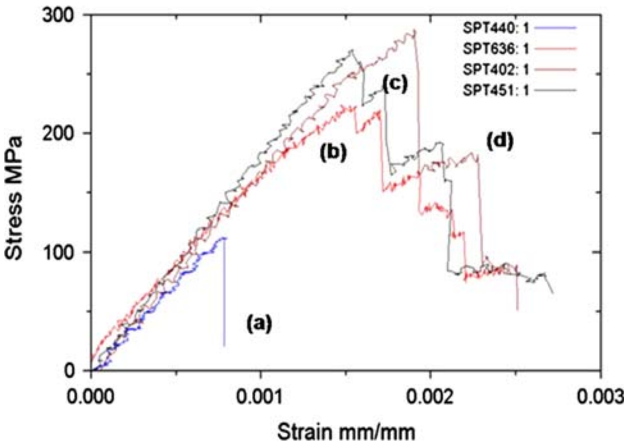

Fig. 9 Stress–strain curves of C_f–SiC + ZrB_2 mini-composites with addition of ZrB_2 from 5 to 20%, processed at 1,600 °C

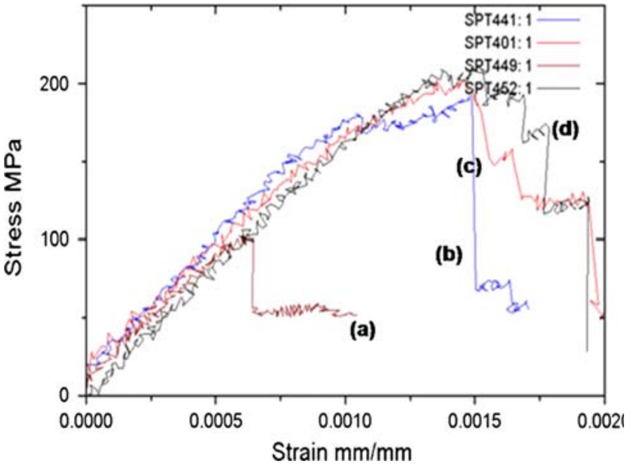

Fig. 10 Stress–strain curves of C_f–SiC + ZrB_2 mini-composites with addition of ZrB_2 from 5 to 20%, processed at 1,700 °C

Figure 9 shows typical tensile stress–strain curves of C_f–SiC + ZrB_2 mini-composites processed at 1,600 °C. The mini-composites exhibit linear stress–strain behavior when ZrB_2 is more than 5% indicating progressive rather than catastrophic failure. Figure 10 shows the stress–strain curves of C_f–SiC + ZrB_2 composites processed at 1,700 °C; stress decreases rapidly after the point of maximum load for these composites possessing 5 and 10% ZrB_2, but for mini-composites containing greater than 10% ZrB_2, the failure is gradual. In both the cases (Figs. 9, 10), it can be seen that the mini-composites with ZrB_2 more than 5%, extended elastic deformation is noted at the beginning. Beyond the elastic limit, the applied load results in uniform plastic deformation till the maximum load is reached, after which load drops with increasing displacement, and finally forms a long tail due to fiber de-bonding and their pullout. The observed increase in strength infers that load can still be transferred effectively from matrix to carbon fiber, assuming its interfacial bond strength between fiber and matrix to be appropriate. The cracking of the matrix occurs under tensile load and the width of the observed cracks increases with increase in the applied load together with de-bonding and pull-out of the fibers from the matrix. Figure 11 shows the variation in strength with increasing temperature as well as with amount of the second phase. However, as compared to composites prepared at 1,600 °C, the composites prepared at 1,700 °C exhibit poorer mechanical properties in spite of failure mode bearing the signature of tough material; this may be rationalized on the basis that the interface bonding is strong enough to effectively transfer load from matrix to the fibers. The variation of tensile strength of the composites is mainly controlled by alteration of the interfacial bond strength between fiber and matrix [23]. The damage of fibers, processed at high temperatures, is due to lower interfacial bond strength which in turn leads to strength degradation of composites.

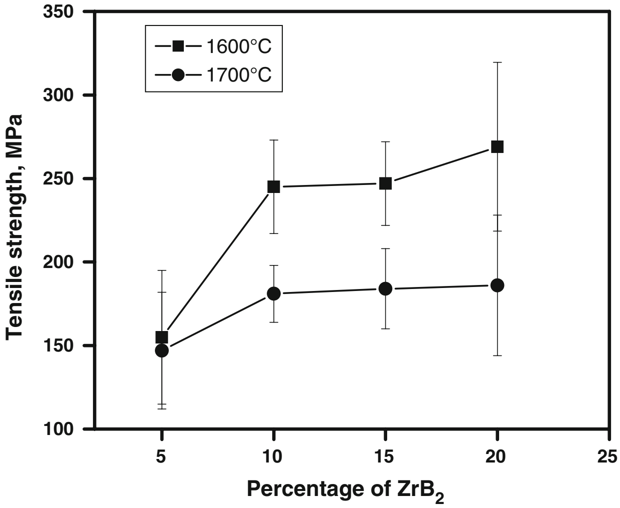

Fig. 11 Variation of tensile strength of C_f–SiC + ZrB_2 mini-composites with percentage of ZrB_2 at two different temperatures

Typical Weibull plots for strength of the carbon fiber reinforced SiC +20% ZrB_2 composites processed at two different reduction temperatures are shown in Fig. 12. Weibull shape parameter indicates the degree of scatter associated with the estimated average strength; a smaller shape parameter indicates larger scatter in strength. The value of Weibull modulus (m) = 3.7 indicates that higher scatter is associated with strength values of SiC + 5% ZrB_2 mini-composite. Weibull shape parameters in axial direction show different values of m, irrespective of the carbon fiber, matrix, and the strength levels. This result indicates that tensile strength obtained using a constant gauge length can be generalized as a measure for the fiber strength, depending on the matrix microstructure.

Figure 13a shows the morphology of the fracture surfaces for the composites processed at 1,600 °C; long fiber pullout is frequently observed, which indicates moderately weak interfacial bond strength. This suggests that no chemical reaction has taken place between the carbon fibers and the matrix at 1,600 °C to cause any fiber degradation. On fracture, the matrix, which is porous and cracked, gets disintegrated leaving the fibers exposed. As indicated in Fig. 13b, the mini-composites prepared at the higher temperature (1,700 °C) show tapered fibers. However, in this case, fiber pullout length is observed to be smaller, and matrix is revealed in between the fibers. It may be inferred that the fiber–matrix interfacial bonding for the composites prepared at 1,600 °C is desirable in comparison to that for the composites prepared at 1,700 °C. This phenomenon could be responsible for the better mechanical properties of the mini-composites processed at 1,600 °C. Examinations of the fracture surfaces of mini-composites processed at 1,700 °C indicate damage of the carbon fibers as the primary mode resulting in lower strength.

The brittle behavior of the mini-composites, prepared at temperatures above 1,600 °C, is considered to be mainly

Fig. 12 Estimation of Weibull modulus of C_f–SiC + 20% ZrB_2 mini-composites processed **a** at 1,600 °C and **b** at 1,700 °C (R = Linear regression and Ps = Survival probability)

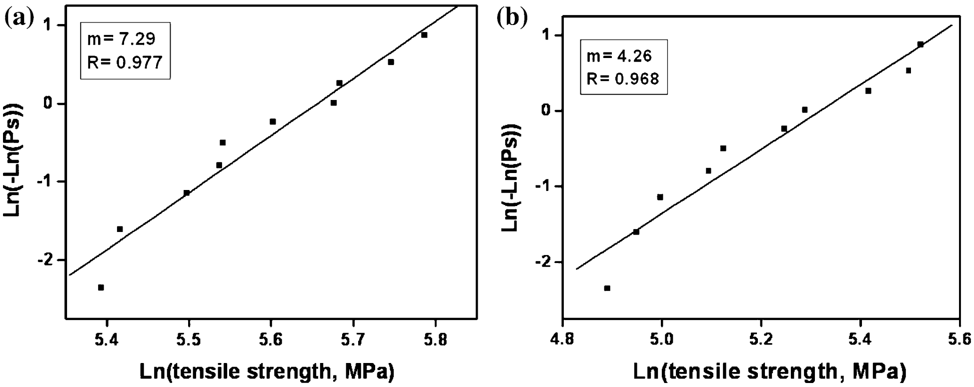

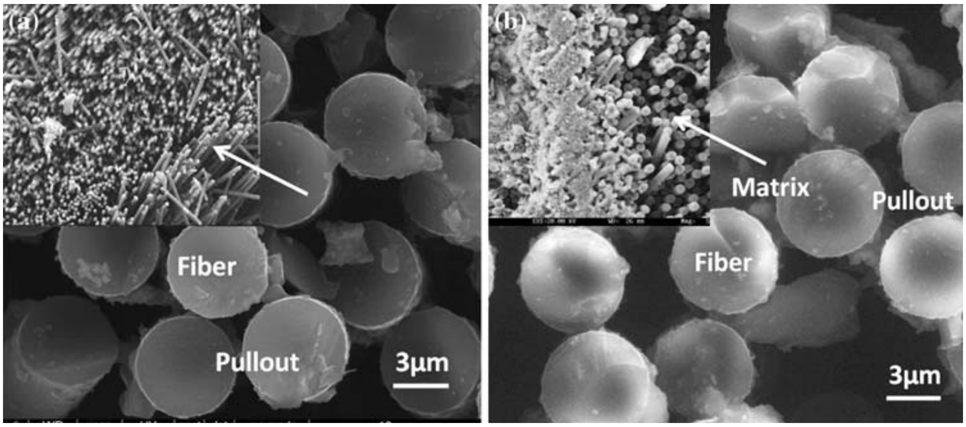

Fig. 13 Fracture surfaces of C_f–SiC + 20% ZrB_2 mini-composites processed **a** at 1,600 °C and **b** at 1,700 °C

due to strengthening of fiber–matrix interface bonding and degradation of the fibers. It is considered that increase in carbothermal reduction temperature promotes diffusion, which degrades the fibers, and strengthens the fiber–matrix interfacial bonding. The effective load carried by fibers depends primarily on their strength and effective area. In C_f–SiO_2–ZrO_2–B_2O_3 system, carbon fiber reacts with ZrO_2 and forms ZrC phase, which leads to stronger interface between fiber and matrix at exposure to high temperature [19]. Irrespective of higher degradation of the fibers in the composites prepared at 1,700 °C compared to that processed at 1,600 °C, it is proposed that the decrease in tensile strength of the composites processed at 1,700 °C is predominantly governed by the strong bonding at the fiber–matrix interface.

Conclusions

Solution-based processing has been used to achieve fine-scale (nanometer-level) mixing of reactants. This method not only lowers the reaction temperature, shortens the soaking time and assists to synthesize ultra fine powders, but also proves to be economical and energy saving. Increase in the driving force arising from amorphous nature of the green powder is considered to be the major reason behind the merits of this process. The process avoids the use of expensive starting materials. The small crystallite sizes, fine particle distribution, and low temperatures to complete carbothermal reductions are indicative of the fine-scale mixing of the reactants in the precursors. This method can be extended to synthesize other metal carbides and borides.

Carbon-fiber-reinforced SiC + ZrB_2 composites have been prepared by the developed soft-solution approach. The X-ray diffraction of the powders and the composites confirms that β-SiC and ZrB_2 form as the matrix phase. However, this reaction would result in the formation of ZrC in addition to ZrB_2 and SiC because of considerable loss of boron oxide from the system at above 1,000 °C. Examinations of the cross-section of the mini-composite shows homogeneous distribution of fibers in the matrix of the mini-composite. The addition of second phase (5–20% ZrB_2) to the matrix improves the strength of the mini-composites. Mini-composites processed at 1,600 °C possess higher density.

The prepared mini-composites exhibit nearly linear stress–strain behavior when mixed with ZrB_2 amounting to more than 10%. It is known that suitable fiber–matrix interfacial bonding is desirable for effective transfer of load from matrix to fibers. The composite processed at 1,600 °C exhibit improved mechanical properties, attributed to desirable degree of fiber–matrix interfacial bonding resulting from the formation of the carbon fiber–matrix interphase such as ZrC. However, composites processed at temperatures above 1,600 °C show degraded mechanical properties, which can be rationalized on the basis of the strongly bonded fiber–matrix interface as well as degradation of the fibers. Further, the differences in tensile strength and fracture energy between C_f–SiC + ZrB_2 composites produced at two different temperatures are attributed to differences in their microstructures and reaction of residual oxides with the fiber. The fiber–matrix bonding due to possible reactions between residual zirconia and the fiber leads to degraded mechanical properties at high processing temperatures.

Weibull statistics support that tensile strength obtained from specimens having constant gauge length can be generalized as a measure of the fiber strength depending on the matrix microstructure. Multiple impregnations and in situ matrix formation have been found to be effective for the development of mini-composites with pseudo-ductile characteristics. The SEM examinations reveal fiber pull-out on the fracture surface of the mini-composites. Investigation of the mechanical properties of the mini-composites at higher temperatures are in progress.

Acknowledgements The authors thankfully acknowledge the financial support received from the Defence Research and Development Organisation, Govt of India in order to carry out this research study. Thanks are also due to SFAG for XRD, and Mr. Rajdeep Sarkar for his valuable help in SEM studies. The authors are grateful to Director, Defence Metallurgical Research Laboratory, Hyderabad for giving permission to publish this article and for his continuous support.

References

1. Naslain R (2004) Compos Sci Technol 64:155
2. Storms EK (1997) The refractory carbides. Refractory materials. Academic, UK
3. Toth LE (1971) Transition metal carbides and nitrides. Academic, New York
4. Upadhya K, Yang JM, Hoffman WP (1997) Am Ceram Soc Bull 58:51
5. Monteverde F, Bellosi A, Guicciardi S (2003) Mater Sci Eng A 346:31
6. Tripp WC, Davis HH, Graham HC (1973) Ceram Bull 52(8):612
7. Ohzawa Y, Takahashi M, Sugiyama K (1997) J Mater Sci 32:4289. doi:10.1023/A:1018659520333
8. Tanaka T, Tamari N, Kondoh I, Iwasa M (1995) J Ceram Soc Japan 103:1
9. Krenkel W (2001) Ceram Eng Sci Proc 22(3):443
10. Subrahmanyam J, Mohan Rao R, Ghosal P, Vijay Kumar M (2004) Indian Patent: 406/DEL
11. Padmavathi N, Subrahmanyam J, Ghosal P, Ray KK, Sweety Kumari (2008) J Mater Process Technol 204(1–3):434
12. Larsen DC, Stuchly SL (1990) In: Mazdiyasni KS (ed) Fiber reinforced ceramic composites, materials, processing and technology. Noyes, Park Ridge, NJ
13. Gonczy ST, Sprandel RC, Faber KT, Robert R (1997) Ceram Eng Sci Proc 18(3):729
14. Naslain R, Lamon J, Pailler R, Bourrat X, Guette A, Langlais F (1999) Compos Part A 30:537
15. Davidge RW (1979) Mechanical behavior of ceramics. Cambridge University, Cambridge
16. Bokhimi X, Morales A, Novaro O, Portilla M, Lopez T, Tzompantzi F, Gomez R (1998) J Solid State Chem 135(1):28
17. Yan Y, Huang Z, Dong S, Jiang D (2006) J Am Ceram Soc 89(11):3585
18. Chase MW Jr (1998) NIST-JANAF thermo chemical tables, 4th edn. American Institute of Physics, Woodbury, NY
19. Weimer AW (ed) (1997) In: Carbide, nitride and boride materials synthesis and processing. Chapman and Hall, London
20. Zhou GH, Wang SW, Guo JK, Zhang Z (2008) J Eur Ceram Soc 28(4):787
21. Rice AG (1985) Ceram Eng Sci Proc 6:589
22. Kim JK, Mai YW (1993) In: Chou TW (ed) Structure and properties of fiber composites, materials science and technology: interfaces in composite, vol 13. VCH, Weinheim, p 239
23. Bobet J-L, Naslain R, Guette A, Ji N, Lebrun J-L (1995) Acta Metall Mater 43:2255